Spectroscopic techniques for the characterization of the YAG:Ce,Gd phosphors and PDMS-YAG:Ce,Gd composites

V. ȚUCUREANU[a,b,*], A. MATEI[a], M. C. POPESCU[a], I. MIHALACHE[a], A. AVRAM[a], B. C. ȚÎNCU[a], M. AVRAM[a], D. MUNTEANU[b]
[a]*National Institute for Research and Development in Microtehnologies (IMT-Bucharest), Erou Iancu Nicolae Street, 126A, 077190, Bucharest, Romania*
[b]*Transilvania University of Brasov, Department of Materials Science, 29 Eroilor Blvd, 500036, Brasov, Romania*

Increasing electricity consumption along with increasing pollution degree has led to the search for alternatives both for electricity generation and for general lighting. In this context, starting with the discovery of the blue LED chips in 1994, solid-state lighting devices were developed using white LEDs obtained by combining blue chips with a YAG:Ce phosphor. Global research in the field of improving the luminescence properties of YAG:Ce phosphors is primarily intended to improve chromaticity coordinates, color rendering index and light efficiency by shifting the spectrum to red and for increasing light conversion efficiency. In this paper we present a co-precipitation method for improving of the optical properties of YAG:Ce phosphors by codoping with Gd^{3+} ions, and embedding in a PDMS matrix for the development of solid-state white light emission device. From a structural point of view, it was confirmed to obtain a phosphor with crystalline garnet structure and confirm the incorporation of phosphor into the PDMS matrix. Fluorescence spectroscopy revealed a spectral shift towards red as well as increase of the quantum yield, both for the Gd codoped phosphor and for the polymeric composite. Spectroscopic methods of analysis confirm the obtaining of a phosphor and a composite with improved properties for optoelectronic applications.

(Received January 7, 2019; accepted August 20, 2019)

Keywords: Phosphor, YAG:Ce,Gd, Composite, PDMS-YAG:Ce,Gd, White LED

1. Introduction

The increase in electricity consumption, of which a significant part (~20-30%) is used for street, commercial, industrial and domestic lighting, has led to the need to find new sources for artificial lighting with the lowest energy consumption. In this context, the generation of white light in an LED by using blue or UV chips together with one or more corresponding phosphors has become a viable alternative to classical lighting systems [1, 2]. However, the practical application of this idea at the industrial level raises several problems, mainly related to the synthesis of luminescent materials and deposition of them onto the blue chips. At the international level, the research in the field of improving the luminescence properties of YAG:Ce phosphors is primarily aimed at improving chromaticity coordinates, color rendering index and light efficacy by shifting the spectrum to red wavelength, and concomitantly increasing the light conversion efficiency. In this respect, the optical properties of the phosphors have been modified by optimizing the synthesis parameters of the technological processes and by using the additional codopants, oxide powders, quantum dots, metal nanoparticles etc [2-11]. One of the modalities of shifting the spectrum can be achieved by the addition of codopants. Considering a phosphor with the molecular formula $(Y,Ce,A)_3(Al,B)_5(O,C)_{12}$, where A is the metallic cation that can replace Y ion from YAG (i.e: A codoping ions: Tb, Gd, Pr, Sm, La, Sr, Ba, Ca etc), B is the metallic cation that can replace Al ion from YAG (i.e: B codoping ions: Si, Ga, Ge, B, P etc), C is the anion that can replace O ion from YAG (i.e: C codoping ions: F, Cl, N, S etc) [12-14]. Codoping can be done with one, maximum two co dopants. The substitution of some YAG components with other ions from the same group (Lu^{3+}, La^{3+}, Gd^{3+} that can substitute Y^{3+} and Ga^{3+}, In^{3+} for Al^{3+} substitution) is a common practice for modifying cerium ion d-f emission. Codoping with Gd, Mg, Si,Ti etc ions can lead to spectral shifts to red, while adding Ga or In ions can lead to a blue shift. This shows a deviation of the network from the cubic symmetry. The use of trivalent rare earth (Eu, Sm, Pr) allows for a spectral shift towards red due to the f-f transitions. But these transitions are much weaker than the d-f transitions of the Ce^{3+} ion in the YAG matrix, and it is concluded that for each codopant a specific radiation is required, for example in case of YAG:Ce,Sm a chip that emits at 404 nm it is necessary in order to obtain promising results. Codopants such as Gd^{3+} lead to a shift in the emission spectrum to higher wavelengths compared to YAG:Ce phosphor, while for Pr^{3+} codoping an emission spectra characterized by two spectral bands - a specific Ce^{3+} (at about 530 -540 nm) and a specific Pr^{3+} (at about 610-640 nm) confirms the possibility of introducing the red component into the white light emission. Also, doping

with Tb^{3+} leads to the appearance of a new sharp band, alongside the Ce^{3+} band in the red spectral field [13-21]. In some cases, formation of allotropic phases has been observed, leading to the alteration of the luminescent properties (i.e: substitution of Y^{3+} with Gd^{3+} may lead to the formation of $GdAlO_3$-perovskite). Another consequence of adding codopants is the decrease in emission intensity due to the diminishing of the YAG phase. These spectral shifts as well as the decrease of the emission intensity represent both an advantage and a disadvantage; therefore the research continues to focus on finding a balance or finding new solutions for the improvement of the emissivity properties of yttrium phosphors [16, 22].

For the development of a white LED it is necessary to deposit the phosphor on the GaN electroluminescent structure, but this is another stage that raises many problems that can influence the quality of the white light emitted. Uniformity, thickness, density of deposited phosphorus layer, distance from the blue structure etc. are important factors for obtaining high quality lighting sources. Also, the adhesion of the phosphor layer is an important factor, because poor adhesion can lead to phosphor dislocation during the manufacturing process or may lead to a lower lifetime of the illumination source. Yet, the biggest problem remains the agglomeration tendency of the phosphor particles regardless of the chosen matrix, due to which problems arise related to the control of the deposited layer thickness and the dispersion/ concentration of the phosphor in the matrix.

For the moment, there are two possibilities of depositing phosphors on the LED chips: (a) depositing phosphors directly on the chips - it is the most commonly used method in the development of white LEDs where the main disadvantage is the low light conversion efficiency due to the fact that some of the light still remains trapped between the phosphor layer and the chip; (b) phosphors deposition on the encapsulated electroluminescent structure - it was found that by keeping a certain distance (i.e.: 0.7 mm) between the structure and the phosphorus it reduces the likelihood that phosphorescence is absorbed by the structure and thus improves phosphors efficiency. To improve the extraction of the light emitted by the semiconductor chip and the phosphor, encapsulations with different geometries were used, each being adapted to the intended application since the angle of light emission is greatly influenced by the geometry of the capsule [23-27]. The development of nanocomposites by embedding phosphor particles into different types of polymeric matrices aims to ensure the dispersion of phosphor in an environment to allow deposition on the chips while maintaining the properties of the luminescence or even improving them. Polymers used as matrices in the development of white light devices need to be transparent and not absorb in the visible field. When choosing a polymeric matrix, the mechanical, chemical, thermal, transparency and transparency properties over time should be considered, the refractive index (2.4 for blue structures, 1.8-2 for phosphors and 1.4-1.6 for the most used polymers) etc. The embedding of phosphor into a polymeric matrix involves the formation of a mixture of one or more phosphors and one or more organic compounds, a mixture that will subsequently be deposited over the LED chips [16, 23, 25].

Generally, inorganic-organic composite types are obtained by in situ synthesis or by dispersing (ex situ) the inorganic materials or the filler, in the organic matrix. Typically, a polymer or oligomers solution containing the nanoparticles is deposited on the LED chips followed by a final heat treatment resulting in a composite film. To improve compatibility and to avoid phase separation, it is not necessary to modify the inorganic nanoparticles, but it is often sufficient to find a suitable solvent / cosolvent (i.e: THF, DMF, butanol, hexane, toluene, etc.) [16, 18, 28, 29]. For the embedding of phosphor in an organic matrix, the literature discloses a series of polymers which are transparent and have no visible absorption, such as: PMMA, PDMS, PVA, epoxy resin, PC [16, 18-19, 30-32].

In the present paper we present the stages of development of a phosphor-PDMS composite. To improve the emissive properties of YAG:Ce phosphor we used Gd ions codoping, during to a coprecipitation process. Using ex situ process, we incorporated the phosphor into the PDMS polymer matrix. The usefulness and applicability of phosphor and composite for the development of white light emission sources has been studied in terms of optical, morphological and structural properties.

2. Experimental

2.1. Materials for sample preparation

For YAG:Ce,Gd synthesis by coprecipitation process and for PDMS-YAG:Ce,Gd composite synthesis the following raw materials were used: yttrium nitrate ($Y(NO_3)_3x6H_2O$), aluminum nitrate ($Al(NO_3)_3x9H_2O$), cerium nitrate ($Ce(NO_3)_3x6H_2O$), gadolinium (III) nitrate hexahydrate ($Gd(NO_3)_3x6H_2O$) dimethyl sulfoxide (DMSO, $(CH_3)_2SO$), cetrimonium bromide (CTAB, $(C_{16}H_{33})N(CH_3)_3Br$), ammonia solutions, hexane ($CH_3(CH_2)_4CH_3$) and poly(dimethylsiloxane) (PDMS, $[(CH_3)_3SiO]_2Si(CH_3)_2$). PDMS polymer was prepared from a Sylgard184 elastomer kit (the base and curing agent should be mixed in a ratio of 10:1).

2.2. YAG:Ce,Gd phosphor and PDMS-YAG:Ce,Gd composite synthesis

The technological experiments for the preparation of YAG:Ce,Gd and PDMS based composites were carried out in two stages. In the first step, coprecipitation of metal cations from nitrates solution (25 mM) using urea, in basic medium, as precipitation agent was used for the synthesis of YAG:Ce,Gd phosphor. For better control of morphology, CTAB (5mM) was used. Stoichiometric quantities of nitrates were used to synthesize a phosphor with molecular formula $(Y_{0.93}Ce_{0.02}Gd_{0.05})_3Al_5O_{12}$. In order to ensure a quantitative precipitation of the cations, an excess precipitate agent was used (molar ratio of nitrates:

urea = 1: 3). DMSO was used to partially replace water from the system due to a much higher boiling point (189°C), thus avoiding surface defects (i.e: pores) as a result of slower evaporation. After the maturation step, the precipitate is filtered and subjected to thermal treatment: presintering up to 400°C for slow evaporation (1-3°C/min) of liquid components, decomposition of nitrates, decomposition of organic compounds and the possibility of eliminating all secondary reaction products under optimum conditions. The final heat treatment of the process is carried out at 1200°C for 6h. In the second step we developed the composite by embedding the phosphor into a PDMS polymer matrix. For better adhesion to the particular polymer interface, and for the separation of the YAG:Ce,Gd powder, we dispersed the phosphor powder in hexane solvent, in a ratio of 1:20 and ultra-sonication. The solvent used allows lower viscosity and better composite handling. The powder thus treated is added to the PDMS base and mixed for 10 minutes, followed by the addition of the second component, the crosslinking agent. Continue stirring for another 15 min., followed by insertion into a vacuum until all the bubbles formed are broken, about 1h. The composite thus obtained is preferably to be used within 12 h of preparation. Addition of crosslinking agent to the mixture followed by thermal treatment at 70°C for a maximum of 12 h resulted in the crosslinking of PDMS chains.

2.3. Characterization of YAG:Ce,Gd and PDMS-YAG:Ce,Gd samples

The YAG:Ce,Gd and PDMS-YAG:Ce,Gd phosphor samples were studied from structurally and optically point of view. Using a Bruker Optics Tensor 27 FTIR spectrometer equipped with an ATR Platinum holder was study the track changes in the kinetic behavior of bonds. All spectra were taken at room temperature, in the wavenumber 4000-400 cm^{-1} range by averaging 64 scans and a resolution of 4 cm^{-1}. FLS920 Edinburgh spectrometer allowed the comparison of luminescent properties for YAG:Ce,Gd phosphor and PDMS-YAG:Ce,Gd composite samples. The photoluminescence (PL) spectra of the phosphors were taken at room temperature using a 450 W Xenon lamp as an excitation source, and a red sensitive - photodetector, in the range of 250-800 nm. The excitation wavelength was at 450 nm. The morphology and dispersion of powders in PDMS was observed with an FEI Nova NanoSEM 630 system.

3. Results and discussion

3.1. Structural characterization

Cross-linking was studied by vibrational spectroscopy using FTIR spectroscopy. Figure 1 shows the spectra of YAG:Ce,Gd powder and PDMS-YAG:Ce,Gd composite samples, and for a better comparison we added the PDMS spectrum.

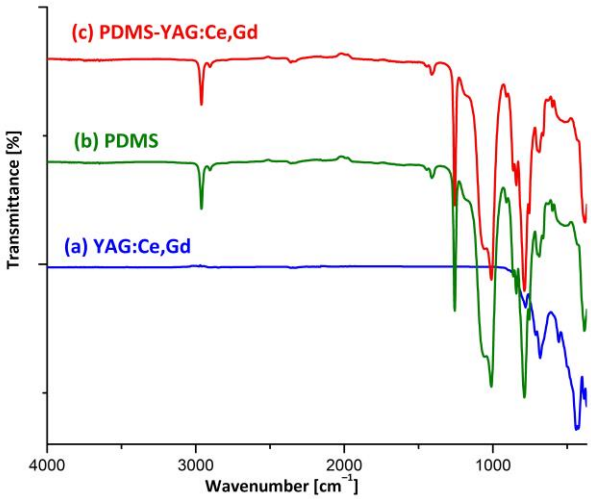

Fig. 1. FTIR spectra for (a) YAG:Ce,Gd powder after annealing at 1200°C, (b) PDMS and (c) PDMS-YAG:Ce,Gd composite

The ATR-FTIR spectrum of the phosphor sample confirms the transition from the amorphous state to the crystalline due to the occurrence of the bands assigned to the M-O bonds. The structure of the unit cell for YAG phosphor is confirmed by spectral bands that can be assigned to the vibration mode of the Al-O bonds from octahedrons centered on Al (AlO_6^{9-} group), by peak from 781 cm^{-1}, and tetrahedra centered on Al, (AlO_4^{5-} group), by peaks centered at 714 and 683 cm^{-1}. Also, the presence of Y-O bonds from dodecahedra centered on Y (forming a YO_8^{13-} group) at 558 cm^{-1} can be observed. The presence of dopant and codopant was confirmed in the FTIR spectrum by bands centered at 441 cm^{-1} for Ce-O and 426 cm^{-1} for Gd-O, respectively. For phosphor, no peaks attributed to organic residues or initial nitrates were observed. The FTIR spectrum of the PDMS polymer (figure 1b) showed absorption bands that can be assigned to the vibration mode of the bonds: C-H bonds from -$Si(CH_3)$ groups at: 2962 and 2905 cm^{-1} (ν_{as}), 1446 and 1412 cm^{-1} (δ_{as}), 1258 cm^{-1} (w), 864 cm^{-1} (ρ); Si-C bonds from –Si-CH_3 group at 843 (ν), 789 (–Si-C and C-H, ρ) , 756 and 689 cm^{-1} (w); Si-H bonds at 2357, 2145, 910 and 663 cm^{-1}. The characteristic peak at 1011 cm^{-1} appeared due to stretching mode of Si-O bonds from -$(CH_3)_2$Si-O-Si$(CH_3)_2$- groups. By comparison with PDMS sample, the FTIR spectra of the YAG:Ce,Gd-PDMS composite (figure 1c) did not show any appreciable change, thus suggesting the total incorporation of the dispersed phase into the polymer matrix.

3.2. Morphology characterization

The optical properties of the filler, and implicitly of the composite, are strongly determined by the surface morphology. Fig. 2 shows the SEM image for a representative sample of phosphor, characterized by a strong tendency to agglomerate of the YAG:Ce,Gd spherical particles. No surface defects were found and an average particle size of about 50 nm was estimated.

Spherical shape and nanometric particle size favor increased emission intensity due to reduced scattering.

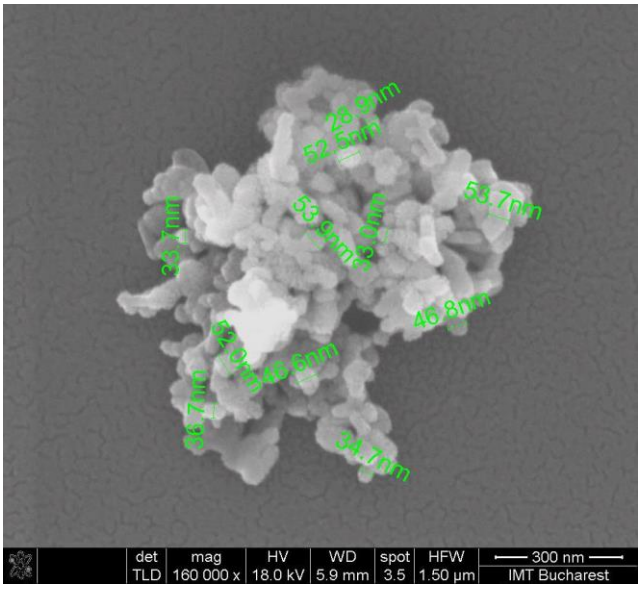

Fig. 2. SEM micrograph for YAG:Ce,Gd powder after annealing at 1200°C

Fig. 3 shows the SEM micrograph for YAG:Ce,Gd filler dispersed in the PDMS matrix.

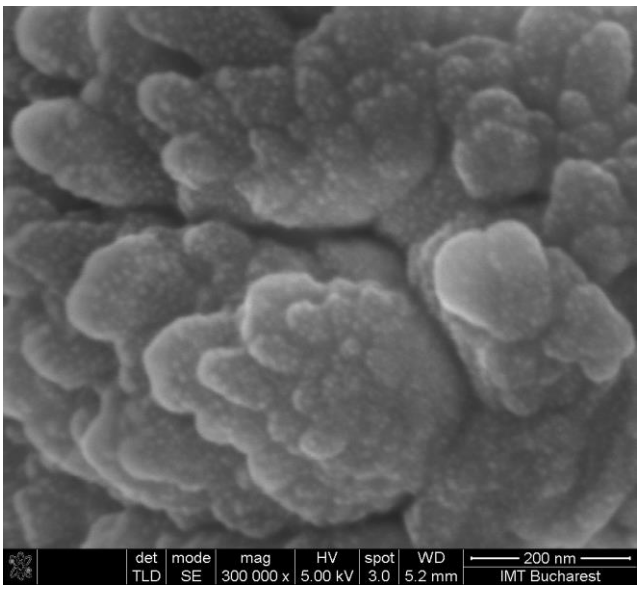

Fig. 3. SEM micrograph for PDMS-YAG:Ce,Gd composite

In the case of the composite sample, dispersion of the phosphor particles inside the polymeric matrix is confirmed, with a decrease in agglomeration tendency, mainly due to the filler dispersion in hexane. No air pockets were observed, the polymer perfectly surrounding the YAG:Ce,Gd particles, suggesting the use of an optimal temperature for polymerization. The phosphor particles were found to have nanometric dimensions and spherical shape without surface defects.

3.3. Luminescence properties

The excitation spectra (recorded at λ_{em} = 550 nm) of the phosphor particles, polymer and composite are shown in Fig. 4. In the excitation spectra, for the phosphor and composite samples, no position variation was found; both spectra are made up of two bands centered at 340 and 450 nm respectively. No band is observed in the pure PDMS, confirming that the spectrum of the composite, as well as the phosphor spectrum, are determined by the transitions due to the Ce^{3+} ion from phosphor and are based on the electron transitions of the type $4f^1 \rightarrow 4f^05d^1$. The presence of Gd^{3+} ion in phosphor leads to the larger bands of the excitation spectra compared to the spectral bands of a YAG:Ce phosphor. The maximum centered at 450 nm confirm the ability of the two types of materials to be used in white light emission by excitement with a blue InGaN chip.

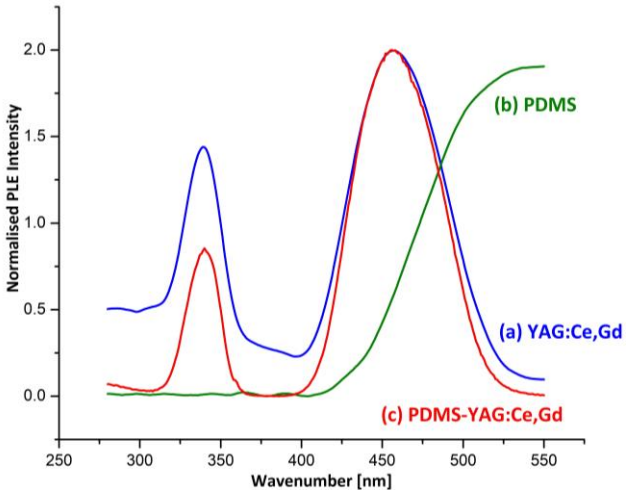

Fig. 4. Photoluminescence excitation spectra for (a) YAG:Ce,Gd powder after annealing at 1200°C, (b) PDMS and (c) PDMS- YAG:Ce,Gd composite

The phosphor and composite emission as a result of excitation at 450 nm are shown in the emission spectra from Fig. 5. In our previous studies, we found that YAG:Ce phosphors are characterized by an emission band centered at about 525-530 nm, but by codoping with Gd^{3+} we succeeded in changing the spectrum by shifting the peak to longer wavelengths. Under these conditions it was found that the emission spectrum for YAG:Ce, Gd phosphor is characterized by a emission band centered at 541 nm, while in the case of PDMS-YAG composite the emission peak with a maximum at 567 nm was found. For these bands, the cerium ion from the garnet structure is responsible and could be attributed to the electron transition from the lowest crystal splitting component of 5d level to the ground state (4f) of Ce^{3+} splinted in $^2F_{5/2}$ and $^2F_{7/2}$ levels. By comparation with the YAG:Ce emission, the displacement in the codoped phosphor spectrum can be explained by the modification of the lattice parameters due to the substitution of Y ions with those of Gd with higher ionic radius. Due to the ionic radius of the codoping

element, a disturbance of the lattice constant occurs, which causes a rise in covalence and a decrease in the energy difference between the excited and the ground state. The lack of absorption bands in the spectral range over 600 nm confirms the spherical morphology of the phosphor particles. The emission spectra of the two samples (nanoparticles and composite) indicate similar behavior, confirming the existence of the same emission centers and maintaining the optical properties of the phosphor in the polymeric matrix. Improvement of luminescent properties can be observed by shifting in the composite spectrum to the higher wavelengths due to the space that appears around the phosphor particles as a result of the polymer insertion between them, of the slight decrease in agglomeration tendency. Also, an increase in emission intensity has been found because of the reduction of the reabsorption phenomenon due to the decrease of the agglomeration degree.

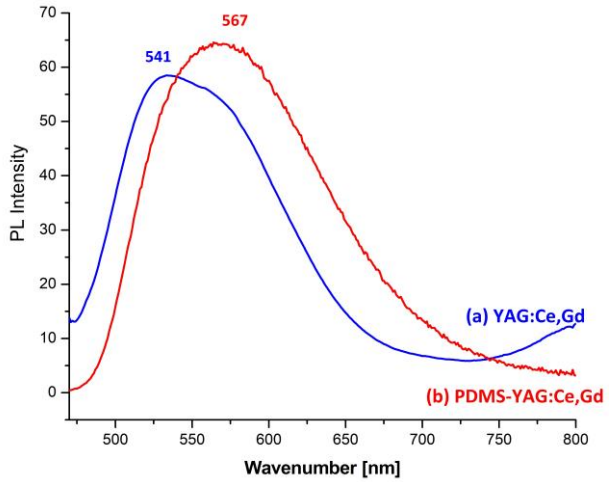

Fig. 5. Photoluminescence emission spectra for (a) YAG:Ce,Gd powder after annealing at 1200°C and (b) PDMS- YAG:Ce,Gd composite

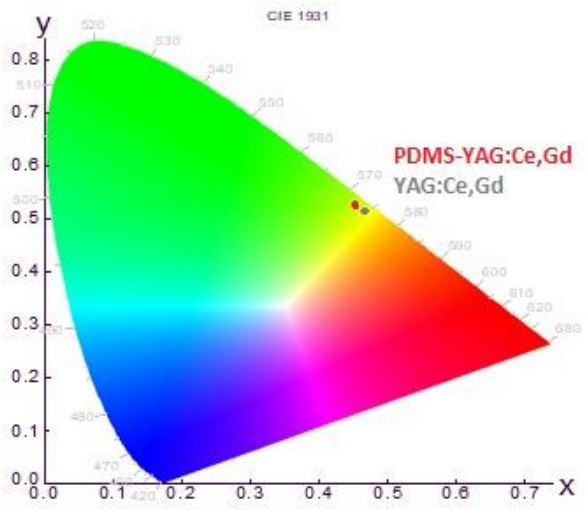

Fig. 6. Color coordinates in the CIE 1931 chromaticity diagram of (a) YAG:Ce,Gd powder after annealing at 1200°C and (b) PDMS-YAG:Ce,Gd composite

The CIE diagram presented in Fig. 6 shows the chromaticity coordinates x,y in the yellow-green field: (0.467; 0.514) for the phosphor sample and (0.447; 0.530) for the composite respectively. For both samples, similar behavior and a high degree of purity of the color confirmed by the intersection points of the x and y coordinates located at the edge of the CIE diagram were found.

Determining the quantum yield for Gd^{3+} codoped YAG:Ce phosphor, upon 450 nm excitation, was found to be 70%. By embedding phosphor particles into the polymer matrix, a significant improvement in luminescence properties was found, as evidenced by the increase in quantum yield to 78.5% for the PDMS-YAG:Ce,Gd sample. The decrease in agglomeration tendency can be translated by improving phosphor emitting properties.

4. Conclusions

YAG:Ce,Gd phosphor particles were obtained by co-precipitation with urea in basic medium and in the presence of CTAB and DMSO followed by a final heat treatment at 1200 °C. After dispersing the powder in hexane, the phosphor was embedded into the polymer matrix of PDMS for the development of the composite. The structural study carried out by FTIR spectrometry confirms the formation of a crystalline phosphor. The ATR-FTIR spectrum for phosphor is characterized by the presence of M-O bonds, where M = Al, Y, Ce, Gd. For the composite, the spectrum highlighted the total incorporation of the YAG: Ce, Gd particles into the polymer matrix. SEM micrograph of phosphor shows the formation of particles with spherical and smooth surfaces at the nanoscale. For the composite, a good distribution of phosphor in the polymeric matrix is observed, with a lower degree of agglomeration and without alteration of morphology. PL excitation and emission spectra confirms the yellow emission of phosphor and the ability to be used with blue chips that emit at about 450 nm for white light generated with a QY of above 70% for YAG:Ce,Gd and 78.5% for composite. Luminescence properties show this type of phosphor to have a yellow light emission centered at 541 nm for YAG:Ce,Gd and 567 nm for PDMS-YAG:Ce,Gd composite. By comparing the properties of YAG:Ce,Gd and fosfor-PDMS composite we can conclude that the modified coprecipitation method presented is a viable alternative to the already known techniques for obtaining the yellow phosphors and the PDMS may be used for phosphor embedding in order to manufacture the white emitting devices.

Acknowledgments

This work was supported by a grant of the Ministry of National Education and Scientific Research, RDI Program for Space Technology and Advanced Research—STAR, project number 639/2017. Also, this work was supported

by UEFISCDI in the Partnership Framework: PN-III-P1-1.2-PCCDI-2017-0214 (Project No. 3PCCDI/2018). Authors would like to acknowledge to researchers: Oana Tutunaru, Carmen Iorga, Tamara Dobre and Marioara Paznicu for cooperation.

References

[1] I. Ahemen, K. De Dilip, A. N. Amah, Appl. Phys. Res. **6**(2), 95 (2014).
[2] L. Su, X. Zhang, Y. Zhang, A.L. Rogach, Top Curr. Chem. (Z) **374**, 42 (2016).
[3] V. Ţucureanu, A. Matei, A. Avram, M. C. Popescu, I. Mihalache, M. Avram, C. Mărculescu**,** B. Ţîncu, M. Volmer, D. Munteanu, MRS Commun. **7**(3), 721 (2017)
[4] T. Hussain, L. Zhong, M. Danesh, H. Ye, Z. Liang, D. Xiao, C. W.Qiu, C. Lou, L. Chi, L. Jiang, Nanoscale **7**(23), 10350 (2015).
[5] S. R. Chung, K. W. Wang, M. W. Wang, J. Nanosci. Nanotech. **13**, 4358 (2013).
[6] D. S. Kong, M. J. Kim, H. J. Song, I. S. Cho, S. Jeong, H. Shin, S. Lee, H. S. Jung, Appl. Surf. Sci. **379**, 467 (2016).
[7] W. H. Chao, R. J. Wu, C. S. Tsai, T. B. Wu, J. Appl. Phys. **107**, 013101 (2010).
[8] E. J. Chung, T. Masaki, Y. H. Song, K. Senthil, M. K. Jung, D. H. Yoon, Phys. Scr. **T157**, 014012 (2013).
[9] P. Sengar, G. A. Hirata, M. H. Farias, F. Castillon, Mat. Res. Bull. **77**, 236 (2016).
[10] C. Tao, P. Li, N. Zhang, Z. Yang, Wang Z, Optik **179**, 632 (2018).
[11] A. Jain, P. Sengar, G. A. Hirata, J. Phys. D: Appl. Phys. **51**, 303002 (2018).
[12] D. Tao, Y.Q. Li,S. Cheng, Patent No. US8133461B2, 2012.
[13] D. Peng, J. Cheng, S. Liming, Q. Qi, G. Guobiao, Z. Xiaoyan, B.Ningzhong J. Rare Earth **35**(4), 341(2017).
[14] H. Shi, J. Chen, J. Huang, Q. Hu, Z. Deng, Y. Cao, X. Yuan, Phys. Status Solidi A **211**(7), 1596 (2014).
[15] V. Schiopu, A. Matei, A. Dinescu, M. Danila, I. Cernica, J. Nanosci. Nanotecho. **12**(11), 8836(2012).
[16] V. Ţucureanu, A. Matei, I. Mihalache, M. Danila, M. Popescu, B. Bita, J. Mat. Sci. **50**(4), 1883 (2015).
[17] X. Zhou, K. Zhou, Y. Li, Z.Wang, Q. Feng, J. Lumin. **132**, 3004 (2012).
[18] T. Guner, D. Koseoglu, M. M. Demir, Opt. Mat. **60**, 422 (2016).
[19] P. J. Yadav, N. D. Meshram, C. P. Joshi, S. V. Moharil, J. Appl. Math. Phys. **6**, 657 (2018).
[20] C. Shen , C. Zhong, J. Ming, J. Exp. Nanosci. **8**(1), 54 (2013).
[21] Y. Yang, J. Li, B. Liu, Y. Zhang, X. Lv, L. Wei, X. Wang, J. Xu, H. Yu, Y. Hu, H. Zhang, L. Ma, J. Wang, Chem. Phys. Lett. **685**, 89 (2017)
[22] C. Shen, K. Li, Q. Hou, H. Feng, X. Dong, IEEE Photonics Technology Letters **22**(12), 884 (2010).
[23] Y. Peng, Y. Mou, X. Guo, X. Xu, H. Li, M. Chen, X. Luo, Opt. Mat. Exp. **8**(3), 605 (2018).
[24] J. H. Oh, S. J. Yang, Y. R. Do, Opt. Express **21**(55), A765 (2013).
[25] H. Luo, J. K. Kim, E. F. Schubert, J. Cho, C. Sone, Y. Park, Appl. Phys. Lett. **86**, 243505 (2005)
[26] J. B. Talbot, J. McKittrick, ECS Journal of Solid State Science and Technology **5** (1), R3107 (2016).
[27] G.Lozano, S. R. K. Rodriguez, M. A. Verschuuren, J. Gomez Rivas, Light: Science & Applications **5**, e16080 (2016)
[28] Lu, Qiaoyu, Synthesis of PDMS-metal oxide hybrid nanocomposites using an in situ sol-gel route, Dissertation, Michigan Technological University (2012).
[29] J. Huang, X. Hu, J. Shen, D. Wu, C. Yin, R. Xiang, C. Yang, X. Liang, W. Xiang, Cryst. Eng. Comm. **17**, 7079 (2015).
[30] M. L. Saladino, A. Zanotto, D. C. Martino, A. Spinella, G. Nasillo, E. Caponetti, Langmuir **26**(16), 13442 (2010).
[31] M. A. Sibeko, A. S. Luyt, M. L. Saladino, Polym. Bull. **74**(7), 2841(2017).
[32] T. Guner, U. Senturk, M. M. Demir, Opt. Mat. **72**, 769 (2017).

*Corresponding author: vasilica.tucureanu@imt.ro; vasilica.schiopu@gmail.com